Raman-induced noiselike pulses in a highly nonlinear and dispersive all-fiber ring laser

Thibault North and Martin Rochette*

Department of Electrical and Computer Engineering, McGill University, Montréal, Québec H3A 2A7, Canada
**Corresponding author: martin.rochette@mcgill.ca*

Received January 16, 2013; revised February 10, 2013; accepted February 12, 2013;
posted February 13, 2013 (Doc. ID 183587); published March 12, 2013

Dual-wavelength noiselike pulses are generated in a fiber ring laser. A first series of pulses is induced at a wavelength of 1550 nm by the interplay of an erbium-doped fiber and nonlinear polarization rotation. From the Raman gain of these pump pulses emerges a second series of Stokes pulses at 1650 nm. With adequate control of the polarization states in the cavity, the noiselike Stokes pulses extend over 84 nm in the Ultralong-wavelengths band (U-band), while the pump pulses span over 46 nm. © 2013 Optical Society of America

OCIS codes: 060.3510, 140.3510, 190.4370, 190.5650, 320.5390, 320.7110.

Ultrashort pulses are generally observed in fiber ring lasers mode locked by saturable absorbers such as in nonlinear polarization rotation (NPR) [1] or semiconductors [2]. In such cavities, another regime of wave packets composed of a picosecond envelope comprising femtosecond-scale oscillations can be triggered as well [3,4]. It is often called the noiselike pulse (NLP) regime and has been recently studied in various cavity configurations that do not always support soliton-like mode locking [5,6]. Spectrally, the averaged noisy pattern corresponding to each of those wave packets can be visualized as a smooth and wide spectrum. Dispersion management, birefringence, and soliton self-frequency shift have been reported to extend that spectrum beyond 100 nm full width at half-maximum (FWHM) [7,8]. Broadband pulses have been generated recently by Vazquez–Zuniga and Jeong in a 22 m long cavity including a segment of highly nonlinear fiber (HNLF) in normal dispersion [9]. Their Raman-extended NLP regime stretched out the spectrum toward longer wavelengths by stimulated Raman scattering (SRS), leading to a 135 nm flat supercontinuum. NLPs are highly energetic and resistant to nonlinear effects [4], and hence have found various applications that take advantage of their broad spectrum, including optical data storage [10], temperature distribution measurements [11], the characterization of fiber Bragg gratings [12,13], and supercontinuum generation [14,15]. As of today, we are aware of only one paper featuring the dual-wavelength operation of a laser in the NLP regime. It was attributed to birefringence-induced loss modulation and was demonstrated using a 450 m long silica cavity, with a spectral offset of 25 nm [4].

In this Letter, we report the observation of a new dual-wavelength fiber ring laser operating in the NLP regime. The laser emits pulses at a wavelength of ~1550 nm, the Raman pump (RP) pulses, from NPR in a cavity comprising an erbium-doped fiber amplifier (EDFA), while pulses at a wavelength of ~1650 nm, the Stokes pulses, are generated from a Raman effect. In [9], the addition of an HNLF increased the amount of SRS experienced by the NLPs, therefore widely broadening their spectrum. By taking advantage of a nonlinear length ~100× shorter than the one proposed in [9], we demonstrate that the action of SRS is reinforced, and instead spawns powerful pulses beyond 1650 nm, outside the amplification region or Er^{3+}-doped silica fibers. In the first regime, an efficient energy transfer from the RP signal to the Stokes signal is observed, such that the Stokes pulses exceed the RP pulse power by 2.5 dB. In the second regime, a flattened dual-wavelength and broadband spectrum is generated, extending up to a wavelength of 1700 nm. To the best of our knowledge, this upper boundary exceeds those of any reported among erbium-doped NLP lasers operating primarily in the C-band [3,4,7,9,14]. The experimental setup schematized in Fig. 1 consists of a ring cavity similar to the ones used for mode locking by NPR [1]. The 1007 m long HNLF has a chromatic dispersion coefficient $D = -0.71\ \mathrm{ps\,nm^{-1}\,km^{-1}}$, a nonlinear waveguide coefficient $\gamma = 11.5\ \mathrm{W^{-1}\,km^{-1}}$, and a loss of 1.5 dB at a wavelength of 1550 nm. The EDFA, which contains an optical isolator, is pumped at 976 nm and has a length × chromatic dispersion product of $\mathrm{LD_{EDFA}} = 138\ \mathrm{ps\,nm^{-1}}$. The other components of the cavity account for ~20 m of silica single mode fiber, and therefore the average chromatic dispersion in the cavity is normal with a value of $\mathrm{LD_{avg}} = -406\ \mathrm{ps\,nm^{-1}}$. An optical spectrum analyzer and a photodiode (PD) are connected at the 1% and 15% output couplers $O_{1,2}$, respectively. The rejection port of the polarization beam splitter (PBS) is also used for monitoring purposes. It provides a linearly polarized laser output with a high output coupling ration (OCR). NLPs are obtained by an adjustment of the two polarization controllers (PCs). With an EDFA pump power of ~100 mW, the sudden broadening of the initial cw regime indicates the presence of a burst of pulses also visible with a fast photodetector. A repetition rate of 194 kHz

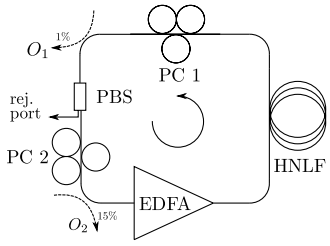

Fig. 1. Ring cavity composed of an HNLF, an EDFA, two PCs, a PBS, and two output tap couplers $O_{1,2}$. EDFA, erbium-doped fiber amplifier; PC, polarization controller; PBS, polarization beam splitter.

is observed at output O_2 for an average power of −5 dBm. Spectra are presented in Fig. 2, along with their time-domain behavior in the corresponding insets. In Fig. 2(a), the PCs are tuned to obtain a pulsed operation around 1550 nm. The spectral bandwidth of the RP signal is 10 nm. A weak signal generated from SRS, noted (i), is also observed. The RP pulses contain most of the power, and NLPs are observed temporally and spectrally. With a further increase of the EDFA gain, both the RP signal and the Stokes signal are raised by a similar amount. We believe that the red-most signal is sustained by a Raman gain supplied by the 1550 nm signal. Indeed, the wavelength separation Ω_1 is of 111 nm, which corresponds well to the 13.2 THz offset expected for a Stokes wave due to an SRS process. In trace (*h*), the PCs have been carefully adjusted to maximize the Stokes signal. The latter contains 1.5 times more energy than the RP signal and has an FWHM of 8.4 nm. A peak is also observed at a wavelength of 1464 nm. Its spectral separation of 95 nm with respect to the RP again has a consistent spectral offset for an anti-Stokes Raman peak. We note that the 50 dB difference between the Stokes and anti-Stokes lines is also expected because of a much less probable phase matching of the anti-Stokes wave [16]. The presence of this peak confirms that the strong gain observed at the Stokes wavelength of the spectrum is due to an SRS process rather than four-wave mixing, which, acting alone, would lead to a pair of new frequency components of similar amplitude. An exact measurement of the peak power of NLPs is difficult to achieve due to their complex structure. However, the NLPs yield to a significant SRS process that exceeds the expected Raman threshold of $P_{\text{th}} = 16A_{\text{Eff}}/(g_R L_{\text{Eff}}) = 14.5$ W, with $g_R = 6.5 \times 10^{-14}$ m W^{-1}, $L_{\text{Eff}} = 850$ m, and $A_{\text{Eff}} \sim 50$ μm^2 for the HNLF [16]. This is a lower bound to the actual NLP peak power. Figure 3 shows the typical frequency-resolved optical gating (FROG) spectrogram of the RP NLPs of Fig. 2(a). The ratio of the autocorrelation peak and the

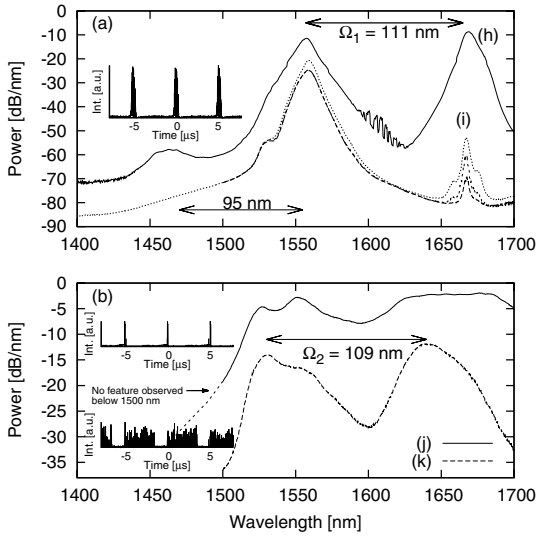

Fig. 2. (a) Dual-wavelength lasing at O_2 at various EDFA pump powers. Inset: PD response of the RP pulses of trace (*h*). (b) Other PC configurations. The spectral offset between the pump and the Stokes pulses are denoted by $\Omega_{1,2}$. Insets: corresponding PD intensity response.

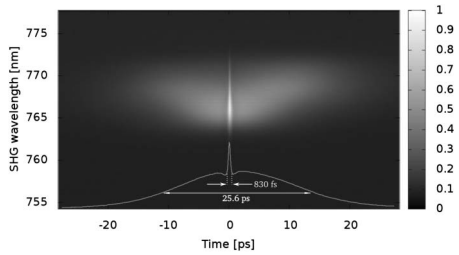

Fig. 3. FROG spectrogram of a NLP and its autocorrelation width of 25.6 ps.

shoulder of the pulse's autocorrelation is close to 2, which indicates the absence of structure in the pulse as discussed, for example, in [3,15]. In Fig. 2(b), other positionings of the PCs lead to two different broadband NLP regimes. The spectrum is shifted toward shorter wavelengths with respect to the spectrum shown in (a). Also, a spectral offset $\Omega_1 \simeq \Omega_2$ is observed. In (*k*), the bandwidth for the RP and the Stokes signals are of 34 and 32 nm, respectively, reflecting that NLPs are also spawned at the Stokes wavelength. In this configuration, the average power of the Stokes pulses is 1.65 times the average power of the RP pulses. With a careful tuning of the PCs, the bandwidth of the RP and Stokes pulses is altered [17]. Stokes pulses with a bandwidth of 84 nm FWHM could be observed as depicted in trace (*j*), extending from 1616 to 1700 nm, while the RP pulses were of 46 nm FWHM. From this point, we focus on what is found to be the most stable regime, denoted (*k*) in Fig. 2(b), often the first one observed when pulsing starts. In Fig. 4(a), the output power at O_2 and the rejection port are presented as functions of the EDFA pump

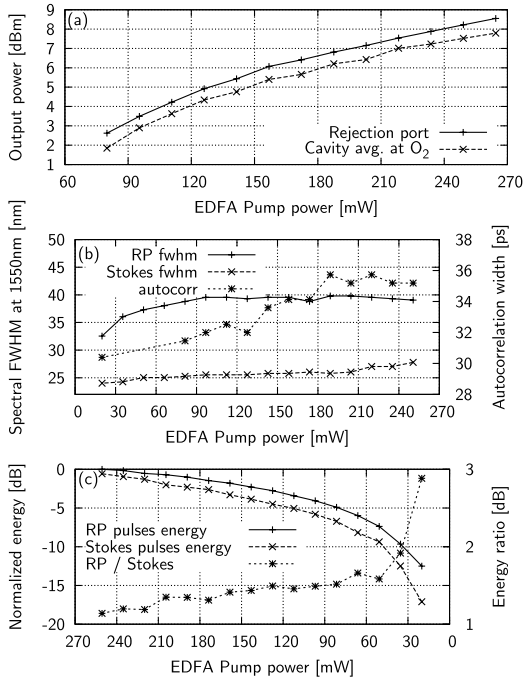

Fig. 4. Effect of a variation of the EDFA pump power. (a) Power at the rejection port and in the cavity, observed from output coupler O_2, (b) spectral width at the RP and Stokes pulses and autocorrelation width for the RP pulses, (c) pulses' spectral energy as the EDFA pump power is decreased.

power. The rejection port presents an OCR of 50% at any EDFA pump power. In Fig. 4(b), an increase of the EDFA pump power leads to a spectral broadening of the RP pulses up to a pump power of 161 mW. After that point, we note that the Stokes pulses take advantage of the additional RP power and undergo spectral broadening as well. In this process, the autocorrelation width of the RP pulses does not significantly change. As opposed to the behavior observed in [9] where the existing NLPs consumed the excess of EDFA pump power and temporally broadened with an increasing EDFA pump power, this rather suggests a transfer of the RP pulse power to new trains of NLPs and to the Stokes pulses via SRS. The energy contained in each of the RP and Stokes pulses is depicted in Fig. 4(c) as the EDFA pump power is decreased. Due to the quasi-instantaneous Raman response [16], the Stokes pulses are sustained only if the RP pulses keep a sufficient peak power. In accordance with time-domain observations, the peak power of the RP pulses diminishes, which quickly lowers the Raman gain and affects both the energy and the spectral peak power of the Stokes pulses. In the time domain, two main regimes are observed at the repetition rate of the cavity, 194 kHz. First, "square-shaped" pulses, also seen in [9], are broadening with increasing EDFA pump power. A PD covering the range 1.2–2.6 μm indicates, as expected, that the Stokes pulses overlap the RP pulses. This was confirmed by alternately filtering each in the spectral domain. Between the RP and Stokes pulses, the group velocity mismatch delay in the HNLF is of 4 ns. This delay is compensated by an asymmetrical gain and loss profile experienced by the slower Stokes pulses. Also, a chaotic regime presented in Fig. 5 indicates a ~3.5 μs long burst that contains a set of impulses separated by ~33 ns. A frequency analyzer indeed shows peaks at the fundamental frequency and at 30 MHz, regardless of the EDFA pump power. For this regime, decreasing the EDFA pump power decreases the burst duration, peak, and average power of the pulses in the cavity. However, at least one powerful RP pulse is always present, providing a sufficient Raman gain to sustain Stokes pulses. As the power is reduced, it is observed that two wavelengths oscillate at the RP with an offset of 8 nm, and pulses slide along each other as observed previously in [4]. This behavior is attributed to the significant birefringence of $\Delta n = 3.5 \times 10^{-7}$ in the HNLF, along with an additional polarization group delay induced by the PBS.

We have demonstrated a dual-wavelength pulsed all-fiber laser based on NPR in the NLP regime. In the presence of an HNLF with a normal dispersion, pulses are observed at the RP frequency in the C-band and at the first Stokes wavelength in the U-band. Although the fundamental cavity repetition rate is in the kHz range, an increase of the EDFA pump power extends the burst duration over the whole cavity period with little change of the spectrum. A broadband continuum of 84 nm FWHM was observed, containing most of the spectral power and spanning from 1616 to 1700 nm, filling the gap between the erbium and thulium emission regions, and hardly accessible by other means. A large OCR of ~50% was observed at the linearly polarized output of the cavity.

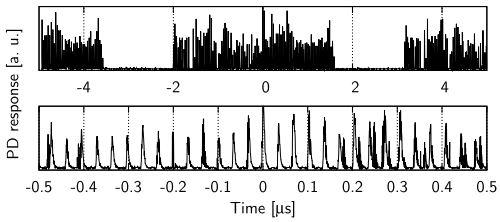

Fig. 5. Time-domain behavior at two different time scales. PD, photodiode.

The authors are thankful to S. Bourquin for insightful comments and the National Optics Institute (INO) in Quebec City for their financial support.

References

1. V. Matsas, T. Newson, and M. Zervas, Opt. Commun. **92**, 61 (1992).
2. S. Y. Set, H. Yaguchi, Y. Tanaka, and M. Jablonski, J. Lightwave Technol. **22**, 51 (2004).
3. M. Horowitz, Y. Barad, and Y. Silberberg, Opt. Lett. **22**, 799 (1997).
4. M. Horowitz and Y. Silberberg, IEEE Photon. Technol. Lett. **10**, 1389 (1998).
5. S. Kobtsev, S. Kukarin, S. Smirnov, S. Turitsyn, and A. Latkin, Opt. Express **17**, 20707 (2009).
6. S. Kobtsev, S. Kukarin, and Y. Fedotov, Opt. Express **16**, 21936 (2008).
7. J. Kang, Opt. Commun. **182**, 433 (2000).
8. L. Zhao, D. Tang, T. Cheng, H. Tam, and C. Lu, Opt. Commun. **281**, 157 (2008).
9. L. A. Vazquez-Zuniga and Y. Jeong, IEEE Photon. Technol. Lett. **24**, 1549 (2012).
10. S. Keren, E. Brand, Y. Levi, B. Levit, and M. Horowitz, Opt. Lett. **27**, 125 (2002).
11. V. Goloborodko, S. Keren, A. Rosenthal, B. Levit, and M. Horowitz, Appl. Opt. **42**, 2284 (2003).
12. S. Keren and M. Horowitz, Opt. Lett. **26**, 328 (2001).
13. S. Keren, A. Rosenthal, and M. Horowitz, IEEE Photon. Technol. Lett. **15**, 575 (2003).
14. Y. Takushima, K. Yasunaka, Y. Ozeki, and K. Kikuchi, Electron. Lett. **41**, 399 (2005).
15. J. Hernandez-Garcia, O. Pottiez, J. Estudillo-Ayala, and R. Rojas-Laguna, Opt. Commun. **285**, 1915 (2012).
16. G. Agrawal, *Nonlinear Fiber Optics*, Optics and Photonics (Academic, 2007).
17. O. Pottiez, R. Grajales-Coutiño, B. Ibarra-Escamilla, E. A. Kuzin, and J. C. Hernández-García, Appl. Opt. **50**, E24 (2011).